

Nature of weak inter- and intramolecular interactions in crystals

5.* Interactions Na...H—B in a crystal of sodium salt of charge-compensated *nido*-carborane [9-SMe₂-7,8-C₂B₉H₁₀][−]**

K. A. Lyssenko,* D. G. Golovanov, V. I. Meshcheryakov, A. R. Kudinov, and M. Yu. Antipin

A. N. Nesmeyanov Institute of Organoelement Compounds, Russian Academy of Sciences,
28 ul. Vavilova, 119991 Moscow, Russian Federation.
Fax: +7 (095) 135 5085. E-mail: kostya@xray.ineos.ac.ru

The character of electron density distribution in the C₂B₃ open face, the influence of the SMe₂ group on the character of electron density distribution, and the nature of the sodium—anion interaction were studied based on the data of high-resolution X-ray diffraction study of crystals of the sodium salt of charge-compensated *nido*-carborane [9-SMe₂-7,8-C₂B₉H₁₀][−] and quantum-chemical calculations for the Na...H—B-bonded dimer, the isolated [9-SMe₂-7,8-C₂B₉H₁₀][−] anion, and the [7,8-C₂B₉H₁₀]^{2−} dianion. The character of electron density distribution in the C₂B₃ open face is analogous to the electron distribution in the cyclopentadienyl ligand. In *nido*-carborane, a substantial charge redistribution takes place compared to that observed in the *closo* analogs. The topological analysis of the electron density distribution function demonstrated that the cation—anion interactions are determined predominantly by Na...H—B contacts. The total energy of these contacts in the {[9-SMe₂-7,8-C₂B₉H₁₀][Na(thf)₂]₂ dimer estimated from X-ray diffraction data is 11.74 kcal mol^{−1}.

Key words: charge-compensated *nido*-carboranes, isolobality, *nido*-carborane salts with alkali metals, quantum-chemical calculations, Na...B—H contacts, electron density distribution, topological theory of Atoms in Molecules, high-resolution X-ray diffraction study.

Alkali metal salts with anionic 11-vertex *nido*-carboranes are widely used as starting compounds in the synthesis of metallocarboranes.^{2–5} However, their structures both in solution and in the solid state remained unknown until very recently. In the last years, it has been demonstrated that these salts exist predominantly as contact ion pairs both in crystals^{6,7} and in solution.⁸

The coordination mode of cations in anionic *nido*-carboranes depends substantially on the cation size. In lithium salts with the charge-compensated [9-L-7,8-C₂B₉H₁₀][−] anions (L = SMe₂ or NMe₃) and the [7,8-C₂B₉H₁₀]^{2−} dianions, η⁵-coordination at the C₂B₃ open face of the carborane is the main coordination mode, whereas sodium salts are characterized by *exo*-coordination at the B(10)B(11)B(6) face.^{6,7}

In the case of *exo*-coordination, the sodium—anion interaction can be either analogous to interactions in *exo-nido* Os, Ru,^{9,10} and Rh¹¹ complexes with 3c—2e metal...H—B bonds or occur through an interaction of the sodium cation with the electron density localized at the center of the triangular face and on the boron atoms.

* For Part 4, see Ref. 1.

** Dedicated to Corresponding Member of the Russian Academy of Sciences E. P. Serebryakov on the occasion of his 70th birthday.

Actually, the negative charge in carboranes is distributed not only between the hydrogen atoms of the B—H bonds¹² but also over the surface of the triangular face.^{13–15} From the geometric standpoint (Na...B and Na...H distances),⁶ both types of interactions in sodium salts with the [9-L-7,8-C₂B₉H₁₀][−] anion are equally probable. In structural studies^{16,17} of small and medium-sized carborane salts with alkali and alkaline-earth metal cations, it was hypothesized that the cations interact predominantly with boron atoms. In contrast, Na...H—B interactions have been suggested to occur in the [{μ-1,2-[o-C₆H₄-(CH₂)₂]-1,2-C₂B₁₀H₁₄]₂Na₄(thf)₆]_n salt.⁷

To elucidate the character of interactions between alkali metal cations and 11-vertex *nido*-carborane anions and estimate their energies, we carried out the topological analysis of the electron density distribution ρ(r) in terms of Bader's theory "Atoms in Molecules"¹⁸ (AIM) based on high-resolution X-ray diffraction data for the sodium salt of *nido*-carborane [9-SMe₂-7,8-C₂B₉H₁₀][−] with composition {Na(thf)₂[9-SMe₂-7,8-C₂B₉H₁₀]₂ (**1**) and quantum-chemical calculations for the {Na(thf)₂[9-SMe₂-7,8-C₂B₉H₁₀]₂ dimer, which is a fragment of the crystal packing of salt **1**.

Since the sodium ions are coordinated at the lateral face, salt **1** is also of interest from the point of view of the

electron density distribution $\rho(\mathbf{r})$ in the C_2B_3 face of carborane, at which the transition metal atoms are coordinated in *closo* complexes. It should be emphasized that the $[9-SMe_2-7,8-C_2B_9H_{10}]^-$ anion is not only isolobal to the cyclopentadienyl anion but also has the same charge.¹⁹ To estimate the influence of the SMe_2 group on the character of charge distribution in the open face, X-ray diffraction study and quantum-chemical calculations for the contact ion pair, which was found in the crystal of **1**, were supplemented with quantum-chemical calculations for the $[9-SMe_2-7,8-C_2B_9H_{10}]^-$ anion (**2**) and the $[7,8-C_2B_9H_{10}]^{2-}$ dianion (**3**).

Results and Discussion

Molecular and crystal structure. X-ray diffraction study of compound **1** demonstrated that, in the crystal, the $[9-SMe_2-7,8-C_2B_9H_{10}]^-$ anions are linked into centrosymmetric dimers by sodium cations (Fig. 1). Each sodium cation forms shortened contacts with hydrogen and boron atoms (2.34–2.52 and 2.854(1)–3.089(1) Å, respectively) of both *nido*-carborane fragments. The shortest Na...H contacts are observed for the H(10) and H(11) atoms, the first atom being involved in contacts with both sodium cations. The B–H...Na bond angles at the hydro-

gen atoms involved in interactions with the sodium ion are in the range of 96–102°, *i.e.*, deviate substantially from linearity (which is preferable for H bonds). At the same time, the distances from the sodium ion to the center of the B(5)B(6)B(10) face (2.816(1) Å) and the midpoint of the B(10)–B(11) bond (2.763(1) Å) are rather short. In addition to the interactions with the anions, the sodium cations form coordination bonds with two THF molecules. This type of interactions between the sodium cations and the *nido*-carborane anions occurs very often and was observed also in salts of other charge-compensated *nido*-carboranes $[9-L-7,8-C_2B_9H_{10}]^-$ (L = NMe_3 or pyridine)⁶ and is similar to that found in the crystal of the $[\{\mu-1,2-[o-C_6H_4-(CH_2)_2]-1,2-C_2B_{10}H_{14}\}Na_4(thf)_6]$ salt.⁷

Stability of the dimer found in the crystal of **1** was additionally confirmed by the results of quantum-chemical calculations. As can be seen from Fig. 2 and Table 1, the mutual arrangement of the cations and anions, except for the tetrahydrofuran rings, as well as the shortest Na...H and Na...B distances, in the crystal structure are virtually the same as those in the isolated dimer. The B–B and B–C bond lengths in the crystal differ from those in the isolated dimer by no more than 0.01 Å (on the average, 0.001 Å). To the contrary, the differences in the bond

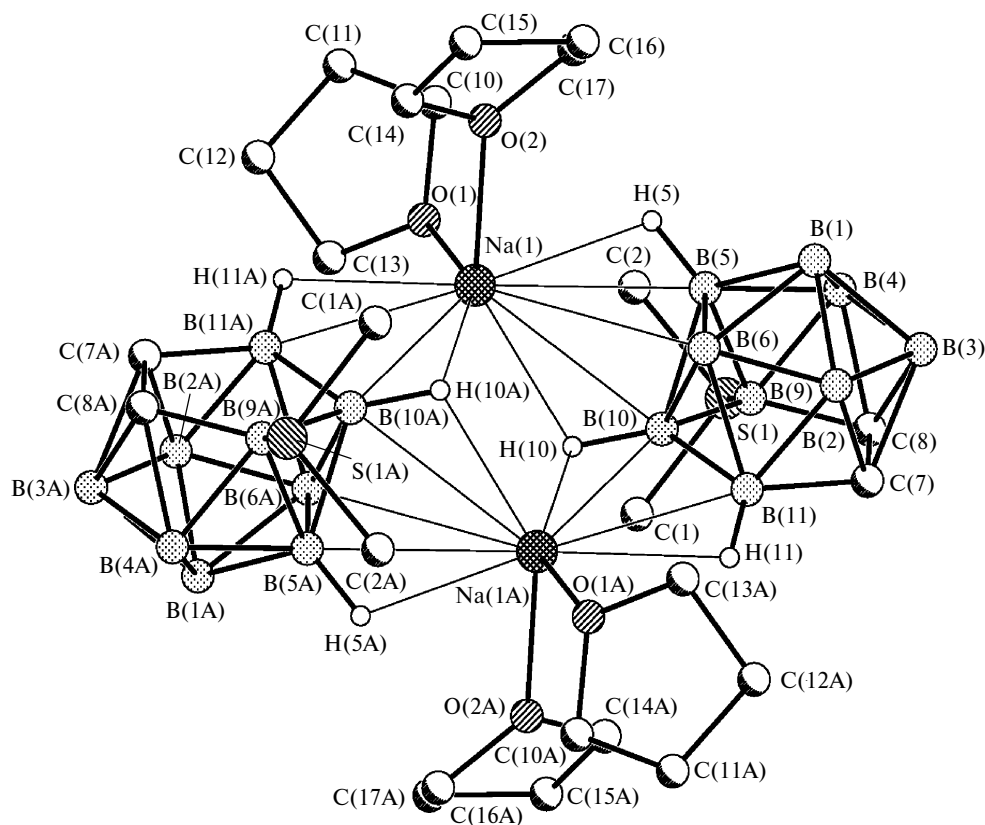


Fig. 1. Overall view of the dimer in the crystal of salt **1**. The hydrogen atoms of the carborane cages, which are not involved in contacts with sodium, are omitted.

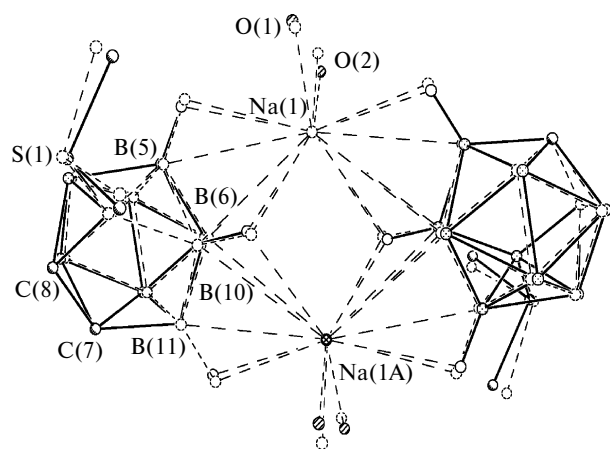


Fig. 2. Superposition of the structures of dimer **1** determined by X-ray diffraction study and the PBE/TZ2p calculations. The carbon atoms of the THF molecules are omitted.

lengths involving the S(1) atom are substantially larger (0.02 Å for B(9)—S(1) and 0.03 Å for C—S). The observed elongation may be associated with both the influence of the polarity of the medium on the formally donor-acceptor B—S bond (see Ref. 20 and references cited therein) and the fact that the C—E and B—E bond lengths (E is a third-period element) calculated by density functional theory are insufficiently accurate, which has been observed earlier²¹ for the Si—C bonds.

An elongation of the B—S bond in the isolated molecule **1** compared to that observed in the crystal is substantially smaller than that generally observed in donor-acceptor boron complexes.²² This fact suggests that the B—S bond is either has a different (nondative) character or is characterized by lower polarity compared to usual donor-acceptor bonds involving the boron atom. Another distinguishing feature of the B—S bond is that its length is independent of the nature of the substituents in *nido*-carborane. For example, the B(9)—S(1) bond length in salt **1** (1.8816(9) Å) is close to the corresponding bond length in the neutral *nido*-carborane 9-SMe₂-7,8-C₂B₉H₁₁ (1.884(2) Å)²³ and is only slightly smaller than the B(9)—S(1) bond lengths in the *closo*-metallo-carborane complexes (1.900(2)—1.921(3) Å).^{19,24}

The main geometric parameters of the carborane fragment in the contact ion pair are also close to the corresponding characteristics in the isolated anion. Small differences (0.009—0.014 Å) are observed for the bonds, which are involved to a greater or lesser extent in interactions with the sodium cations. However, the B(10)—B(11) bond, which is involved in interactions with the cations to the most extent, remains unchanged. An analogous situation is observed for the B—H bonds. It can be seen that the bond lengths for the hydrogen atoms, which form shortened contacts with the Na⁺ cations, are systematically shorter in isolated anion **2**. However, an analogous

Table 1. Main geometric parameters of the {[9-SMe₂-7,8-C₂B₉H₁₀][Na(thf)₂Na]₂ dimer (**1**) in the crystal and in the isolated state, of the [9-SMe₂-7,8-C₂B₉H₁₀][−] anion (**2**), and of the [7,8-C₂B₉H₁₀]^{2−} dianion (**3**)

Bond	d/Å			
	1		2	3
	X-ray diffraction	PBE/TZ2p		
C(7)—C(8)	1.5346(9)	1.535	1.539	1.546
C(7)—B(11)	1.617(1)	1.625	1.635	1.628
B(10)—B(11)	1.737(1)	1.741	1.745	1.752
B(9)—B(10)	1.7157(9)	1.724	1.719	1.752
C(8)—B(9)	1.598(1)	1.609	1.606	1.628
C(7)—B(3)	1.721(1)	1.728	1.728	1.734
C(8)—B(3)	1.728(1)	1.733	1.732	1.734
C(7)—B(2)	1.724(1)	1.722	1.726	1.730
C(8)—B(4)	1.723(1)	1.726	1.731	1.730
B(4)—B(9)	1.782(1)	1.782	1.786	1.812
B(9)—B(5)	1.781(1)	1.777	1.783	1.807
B(10)—B(5)	1.792(1)	1.790	1.796	1.794
B(6)—B(10)	1.792(1)	1.790	1.792	1.794
B(6)—B(11)	1.799(1)	1.796	1.805	1.807
B(2)—B(11)	1.800(1)	1.795	1.804	1.812
B(2)—B(3)	1.767(1)	1.768	1.772	1.777
B(3)—B(4)	1.773(1)	1.774	1.776	1.777
B(4)—B(5)	1.784(1)	1.786	1.800	1.769
B(5)—B(6)	1.781(1)	1.780	1.778	1.792
B(6)—B(2)	1.758(1)	1.763	1.760	1.769
B(1)—B(6)	1.811(1)	1.804	1.824	1.820
B(1)—B(5)	1.795(1)	1.795	1.800	1.820
B(1)—B(4)	1.768(1)	1.771	1.767	1.779
B(1)—B(3)	1.762(1)	1.767	1.761	1.754
B(1)—B(2)	1.780(1)	1.782	1.788	1.779
S(1)—B(9)	1.8816(9)	1.898	1.906	—
S(1)—C(1)	1.791(1)	1.826	1.831	—
S(1)—C(2)	1.787(1)	1.828	1.830	—
Na(1)...O(1)	2.2737(7)	2.470	—	—
Na(1)...O(2)	2.3377(7)	2.416	—	—
Na(1)...B(5)	2.9611(9)	2.804	—	—
Na(1)...B(6)	3.089(1)	2.942	—	—
Na(1)...B(10)	2.9477(9)	2.875	—	—
Na(1)...B(10A) ^a	2.9396(8)	3.014	—	—
Na(1)...B(11A) ^a	2.8530(9)	2.903	—	—
B(5)—H(5) ^b	1.207	1.207	1.203	1.211
B(6)—H(6)	1.210	1.210	1.201	1.211
B(10)—H(10)	1.219	1.219	1.212	1.220
B(11)—H(11)	1.212	1.212	1.207	1.218
Na(1)...H(5)	2.526	2.473	—	—
Na(1)...H(6)	2.772	2.649	—	—
Na(1)...H(10)	2.331	2.427	—	—
Na(1)...H(10a)	2.540	2.578	—	—
Na(1)...H(11a)	2.326	2.348	—	—

^a The atoms labelled by A are related to the unlabelled atoms by the symmetry operation 2 − x, 1 − y, z.

^b The C—H and B—H bond lengths in the crystal are normalized to the corresponding bond lengths obtained at the PBE/TZ2p level of theory.

shortening is observed also for the B(6)—H(6) bond, which is not involved in an analogous contact (H(6)...Na(1), 2.72 Å). Therefore, analysis of the geometric parameters does not give an unambiguous answer to the question about the character of the cation—anion interaction in salt **1**.

In addition to the bond lengths in the carborane polyhedron, the arrangement of the SMe₂ group with respect to the open face of the *nido*-carborane and the envelope conformation of the open face with the B(10) atom deviating from the plane through the other atoms also remain virtually unchanged (see below).

The fact that the arrangement of the SMe₂ group relative to the open face of carborane remains constant suggests that these fragments are involved in specific interaction. Actually, the lone pair (Lp) of the sulfur atom of the SMe₂ group is antiperiplanar to the B(9)—B(10) bond in the crystal, in the isolated dimer, and in anion **2** (Lp—S(1)—B(9)—B(10) torsion angles are 163.8, 156, and 162°, respectively). Presumably, charge transfer from the sulfur Lp to the antibonding orbital of the B(9)—B(10) bond takes place in *nido*-carborane [9-SMe₂-7,8-C₂B₉H₁₀][−]. An analogous arrangement of the SMe₂ group relative to the C₂B open face is retained in a series of metallocarboranes. For example, the sulfur Lp of the SMe₂ group in the 3-L-3,3-I₂-4-SMe₂-3,1,2-*closo*-RhC₂B₉H₁₀ complex (where L = CO) is antiperiplanar to the B(9)—B(10) bond, whereas the sulfur Lp is antiperiplanar to the B(9)—B(5) bond in the presence of a bulkier substituent (L = PPh₃).²⁵ Therefore, charge transfer from the Lp of the S(1) atom to the antibonding orbital of the B(9)—B(10) or B(9)—B(5)/B(9)—B(4) bonds can occur depending on the steric volume of the substituent (see also Refs 19 and 24). The antiperiplanar arrangement of the sulfur Lp with respect to the B—C bond was found in none of metallocarboranes.

Presumably, it is the stereoelectronic interaction between the SMe₂ group and the *nido*-carborane cage that is responsible for distortion of the open face, *viz.*, for the deviation of the B(10) atom from the plane. For example, the deviations of the B(10) atom from the plane through the C(7), C(8), B(9), and B(11) atoms in the crystal, the isolate dimer, and anion **2** are virtually equal ($\Delta = 0.075$, 0.072, and 0.079 Å, respectively). However, quantum-chemical calculations for dianion **3** demonstrated that the envelope conformation of the open face is retained in the absence of the SMe₂ group as well. Moreover, the deviation of the B(10) atom in dianion **3** ($\Delta = 0.103$ Å) is even larger than that in salt **1** and anion **2**. It should be emphasized that the distortion is observed only for the open face, whereas, in structures **1**—**3**, the pentagonal B(2)B(3)B(4)B(5)B(6) face located parallel to this open face is planar.

A comparison of structures **2** and **3** shows that the main variations are observed for the bonds involving the

B(9) atom or the atoms directly bound to this atom. The other bonds, including the C(7)—C(8), C(7)—B(11), and B(10)—B(11) bonds of the open face, vary only by 0.007 Å. All bonds in dianion **3** are elongated, whereas the B(4)—B(5) bond is shortened by 0.031 Å.

Therefore, the effect of the SMe₂ group on the character of bond length distribution in both the C₂B₃ open face and the other portion of the polyhedron is predominantly local in character and, apparently, does not lead to a substantial charge redistribution in the open face.

Electron density distribution. Analysis of the electron density distribution in icosahedral *closo*-carboranes have demonstrated^{14,15} that considerable electron delocalization over the surface of the polyhedron leads to a decrease in the electron density at the edges and a considerable charge accumulation on the triangular faces. However, another character of electron density distribution is observed in the *nido*-carborane anion [9-SMe₂-7,8-C₂B₉H₁₀][−] of salt **1**. As can be seen from the deformation electron density (DED) section, there is a substantial charge accumulation in all bonds of the C₂B₃ open face (Fig. 3, *a*); the DED maxima are 0.30—0.35 e Å^{−3}. On the contrary, the DED accumulation in the bonds of the pentagonal B(2)B(3)B(4)B(5)B(6) face is less pronounced (peak heights are smaller and are in the range of 0.10—0.20 e Å^{−3}). The highest peak is observed in the B(3)—B(4) bond, which is located below the C(7)—C(8) bond, whereas the lowest peaks are localized in the B(5)—B(6) and B(5)—B(4) bonds located below the B(9) atom. A decrease in the peak height in the B(5)—B(6) bond can be associated not only with the influence of the SMe₂ group but also with the effect of the sodium cation.

Interestingly, the charge distribution in the open face of the anion in **1** is virtually identical to that in the Cp ligand of vanadocene V(η⁵-Cp)₂.²⁶ There are only the following differences in the DED distribution in the C₂B₃ face and in the Cp ligand: slight differences in the peak heights in the B—B and C—C bonds and the shift of the DED maxima in the B—C bonds toward the carbon atom. The data on the character of electron density distribution show that the open face of the *nido*-carborane is analogous (isolobal) to the Cp ligand.

In the *nido*-carborane anion of **1**, a substantial charge redistribution takes place compared to that observed in the *closo* analog, which is evidenced by analysis of the DED maps in the planes of the triangular faces. Earlier, it has been demonstrated^{14,15} that the BBB faces in *closo*-carboranes are characterized by the uniform DED distribution in the center of the ring. However, as can be seen from the DED sections, this character of electron density distribution in the anion of **1** is retained only for the low belt of the rings involving the B(1) atom (Fig. 4, *a*). In all other rings, the DED maxima are localized predominantly in the bonds of the open C₂B₃ face (see Fig. 4, *b*, *c*).

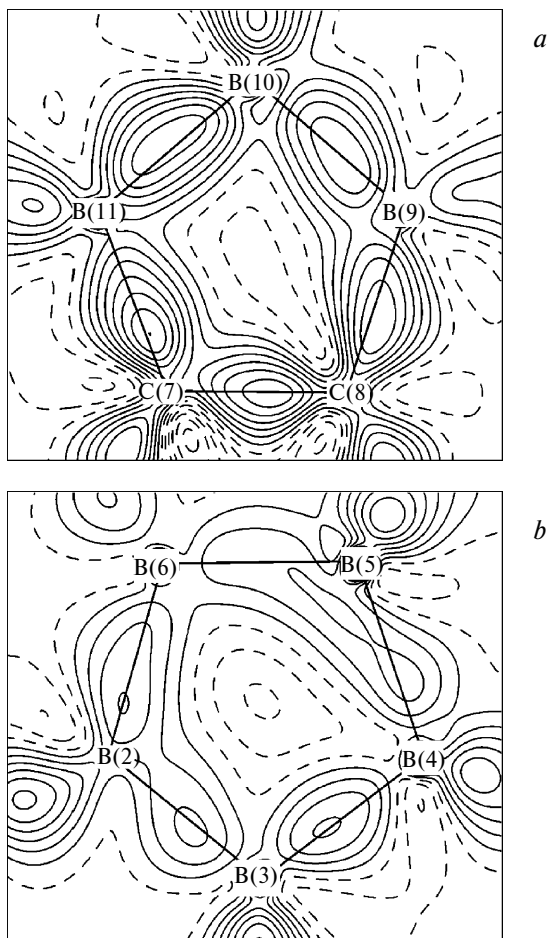


Fig. 3. Deformation electron density sections through the C(7)C(8)B(9)B(10)B(11) (a) and B(2)B(3)B(4)B(5)B(6) (b) planes in the crystal of **1**. The maps are contoured at $0.05 \text{ e } \text{\AA}^{-3}$ intervals. The negative and zero contours are dashed.

As for charge transfer from the SMe_2 group to the antibonding orbital of the B(9)—B(10) bond, analysis of the DED maps allowed only the conclusion that the sul-

fur lone pair is actually parallel to the depletion region located on the extension of the B(9)—B(10) bond line. This is not contradictory to charge transfer, but does not unambiguously support this phenomenon (Fig. 5).

The sections of deformation electron density, as well as of other functions (Laplacian of the electron density, the electron localization function), are least informative in the Na...H interaction region. The DED section passing through the coplanar Na(1), O(1), H(5), and H(6) atoms shows no electron accumulation in the region of the assumed Na...H contact (Fig. 6). Moreover, unlike the Lp of the O(1) atom of the THF molecule, the B—H bond is not polarized.

To obtain additional information on the nature of the sodium—*nido*-carborane anion interactions, we carried out the topological analysis of the electron density distribution.

The same characteristic sets of the critical points were found for the *nido*-carborane anion in the crystal of **1**, the isolated dimer, and anion **2**. As in the carboranes studied earlier,^{14,15} the critical points (3,−1) (CP (3,−1)) corresponding to chemical bonding in terms of the AIM theory¹⁸ are localized in all B—B, B—C, and C—C edges of the polyhedron and also in the C—H, B—H, C—S, and B—S bonds. In turn, CPs (3,+1) are localized on the triangular faces and on the open face of the *nido*-carborane cage, whereas CP (3,+3) is localized in the center of the polyhedron.

The main topological characteristics of the B—B and B—C bonds, except for the bonds of the open face, differ only slightly from those found earlier in *closo*-carboranes.^{14,15} The values of $\rho(\mathbf{r})$ and $\nabla^2\rho(\mathbf{r})$ for the B—B bonds at CPs (3,−1) vary from 0.82 to $0.87 \text{ e } \text{\AA}^{-5}$ and from -2.97 to $-2.43 \text{ e } \text{\AA}^{-5}$, respectively. The corresponding values for the B—C bonds are slightly larger, and they also correspond to shared interatomic interactions. The bonds of the C_2B_3 open face of the *nido*-carborane are characterized by systematically higher values of $\rho(\mathbf{r})$ at

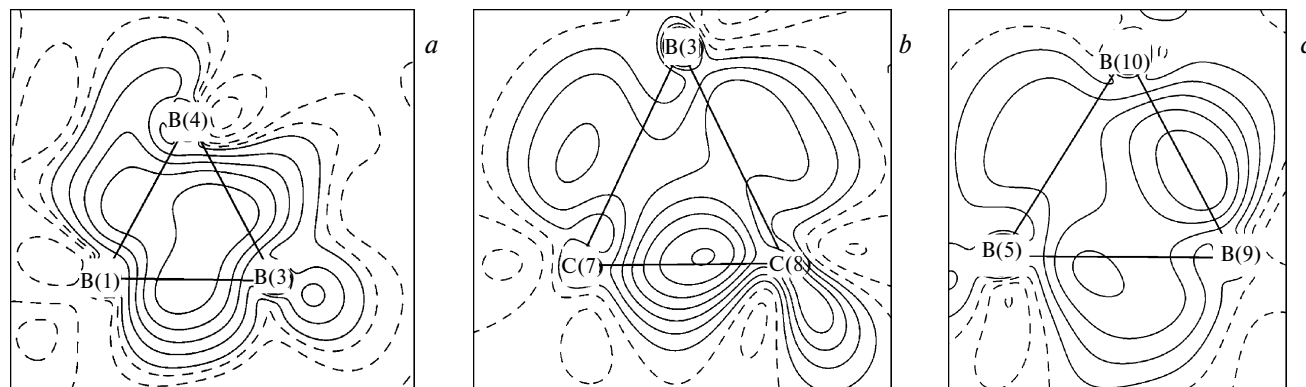


Fig. 4. Deformation electron density in the plane of the triangular faces in the crystal of **1**. The maps are contoured at $0.05 \text{ e } \text{\AA}^{-3}$ intervals. The negative and zero contours are dashed.

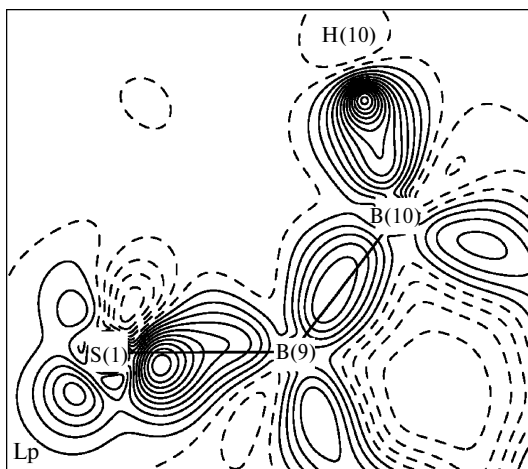


Fig. 5. Deformation electron density in the S(1)B(9)B(10) plane. The maps are contoured at $0.1 \text{ e } \text{\AA}^{-3}$ intervals. The negative and zero contours are dashed.

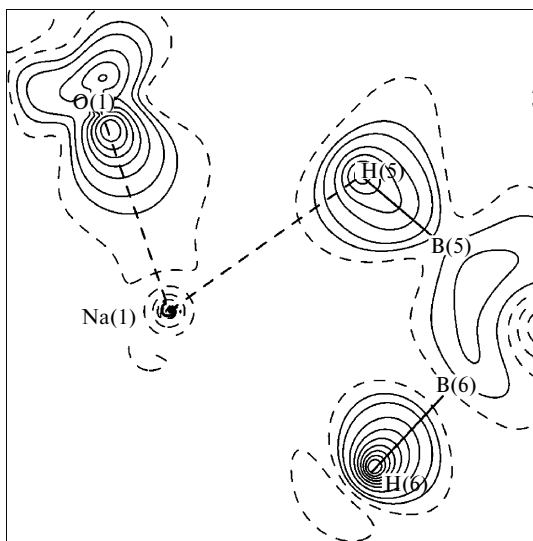


Fig. 6. Deformation electron density in the plane passing through the Na(1), O(1), H(5), and H(6) atoms (coplanar within 0.009 \AA). The maps are contoured at $0.1 \text{ e } \text{\AA}^{-3}$ intervals. The negative and zero contours are dashed.

CPs (3,−1). For example, the values of $\rho(\mathbf{r})$ and $\nabla^2\rho(\mathbf{r})$ at the CPs (3,−1) of the B(10)—B(9) and B(10)—B(11) bonds vary from 0.94 to $0.96 \text{ e } \text{\AA}^{-3}$ and from -5.48 to $-5.38 \text{ e } \text{\AA}^{-5}$, respectively. For the C—B bonds, the values of $\rho(\mathbf{r})$ at the CPs (3,−1) (1.04 – $1.18 \text{ e } \text{\AA}^{-3}$) are comparable with the corresponding value for the C—C bond ($1.23 \text{ e } \text{\AA}^{-3}$) in 1-phenyl-*o*-carborane.¹⁵ Therefore, an increase in $\rho(\mathbf{r})$ at CPs (3,−1) for the bonds of the open face cannot be accounted only for by shortening of the bonds compared to those observed in the *closo* polyhedra (see Table 1).

In turn, the topological characteristics of the C(7)—C(8) bond in molecule **1** also differ substantially from the analogous characteristics in *closo*-carborane, which is manifested not only in a substantial increase in $\rho(\mathbf{r})$ (to $1.55 \text{ e } \text{\AA}^{-3}$) compared to that in 1-phenyl-*o*-carborane ($1.22 \text{ e } \text{\AA}^{-3}$) but also in a decrease in the ellipticity (ϵ) to 0.37 (0.98).¹⁵ Interestingly, the ellipticity ϵ for the C—C bond in molecule **1** is close to the corresponding value for the C—C bonds (0.25) in 3d-metallocenes.²⁷

A decrease in the ellipticity for the bonds of the open face has a general character. In *closo*-*o*-carboranes, the ellipticities ϵ for the B—C and C—C bonds are generally rather high (higher than 2),^{14,15} whereas the ellipticities for the bonds of the open face are in the range of 0.7 – 0.9 .

The B—S bond in the crystal of **1**, unlike those in donor-acceptor boron complexes,²² also corresponds to shared interatomic interactions ($\rho(\mathbf{r}) = 0.95 \text{ e } \text{\AA}^{-3}$ and $\nabla^2\rho(\mathbf{r}) = -7.59 \text{ e } \text{\AA}^{-5}$). Taking into account that the ellipticity of this bond is rather high (0.10), it can be concluded that charge transfer from the sulfur Lp of the SMe₂ group to the antibonding orbital of the B(9)—B(10) bond in *nido*-carborane 9-SMe₂-7,8-C₂B₉H₁₀[−] does take place, resulting in a stable conformation relative to the B(9)—S(1) bond.

Analysis of the contacts of the sodium cation demonstrated that CPs (3,−1) are observed only between the cation and the hydrogen atoms, as well as between the cation and the oxygen atoms of the THF solvate molecules. Of all the Na...H contacts, only the Na(1)...H(5), Na(1)...H(10), Na(1)...H(10A), and Na(1)...H(11a) interactions in the crystal correspond to chemical bonding (see Fig. 1, Table 1). Although $\rho(\mathbf{r})$ at CPs (3,−1) of the Na...H bonds are substantially lower (0.04 – $0.05 \text{ e } \text{\AA}^{-3}$) than the corresponding values for the Na...O contacts (0.16 – $0.17 \text{ e } \text{\AA}^{-3}$), both types of contacts correspond to closed-shell interactions, which is evidenced by the positive values of $\nabla^2\rho(\mathbf{r})$ and the energy densities (0.67 – $1.15 \text{ e } \text{\AA}^{-5}$, 0.0024 – 0.0032 a.u. and 3.06 – $3.64 \text{ e } \text{\AA}^{-5}$, 0.0050 – 0.0066 a.u. for the Na...H and Na...O contacts, respectively).

The formation of Na...H contacts results in the closure of two independent five-membered Na(1)H(10)B(10)B(5)H(5) and Na(1)H(10a)B(10a)B(11a)H(11a) rings related by a center of symmetry and the closure of the centrosymmetric four-membered Na(1)H(10)Na(1a)H(10a) ring. For each ring, CP (3,+1) was found (see Fig. 1). In the latter ring, the position of CP (3,+1) coincides with the center of symmetry.

Taking into account the changes in the Na...H distances in the crystal and in the isolated dimer calculated by the quantum-chemical method (see Table 1), the number of Na...H interactions could also be expected to change. However, the topological analysis of $\rho(\mathbf{r})$ based

on the results of quantum-chemical calculations demonstrated that the molecular graph observed in the crystal is completely retained in the isolated dimer. Therefore, the dimer of **1** is stable, which is determined not only by shortened distances but also, primarily, by the nature of interacting atoms.

In spite of the low values of $\rho(\mathbf{r})$ at CPs (3,−1) of Na...H interactions, their energies estimated from the correlation between the potential energy density and the contact energy^{1,27,28} vary from 1.76 to 1.18 kcal mol^{−1}, and the total energy per cation is 5.87 kcal mol^{−1}. The highest energy is observed for the shortest Na(1)...H(10) and Na(1)...H(11a) contacts (see Table 1). The energy of these contacts is close to that of weak C—H...O contacts²⁷ and is higher than the energies of the C—H...F contacts in the crystal of 2-trifluoroacetyl-5-trifluoromethylpyrrole.²⁸ For comparison, the energy of Na...O interactions calculated according to the same procedure is 7.7 kcal mol^{−1}.

To estimate the contribution of the 3c—2e bonding to Na...H interactions, we also found CPs (3,−1) for the electron density functions for two types of model clusters calculated without consideration of the hydrogen atoms (**A**) and the boron atoms (**B**) involved in contacts with the sodium cation. The clusters **A** and **B** were calculated for each assumed interaction site (boron or hydrogen atom) with the exclusion of this atom from the calculations of the total electron density function. For the clusters **A**, the critical point (3,−1) for the cation—anion interaction disappeared in all cases, whereas CPs (3,−1) for the clusters **B** were observed, but the electron densities at these points decreased by a factor of more than 1.5. Hence, it can be concluded that, although the interaction between the sodium cation and the *nido*-carborane anion [9-SMe₂-7,8-C₂B₉H₁₀][−] in the case of *exo*-coordination is determined primarily by interactions with the hydrogen atoms, the 3c—2e interaction with the B—H bond also makes a contribution to the system under consideration.

The total energy of the Na...H interactions in the crystal of **1** estimated from the X-ray diffraction data is 11.74 kcal mol^{−1}, which is consistent with rather high stability of the cation-anion pairs in solution, which has been demonstrated by NMR spectroscopy.⁸

Experimental

The NMR spectra were recorded on a Bruker AMX-400 spectrometer (400 MHz).

Compound **1** was synthesized under argon with the use of anhydrous solvents. The 9-SMe₂-7,8-C₂B₉H₁₁ compound (973 mg, 5 mmol) was added to a suspension of NaH (200 mg, 8.3 mmol) in THF (20 mL) with stirring using a magnetic stirrer. The reaction mixture was refluxed for 1 h, cooled to room temperature, and filtered. Then light petroleum (40 mL) was added. The white precipitate that formed was filtered off, washed with light petroleum, and dried *in vacuo*. The yield of compound **1** was

1.676 g (93%). ¹H NMR (C₆D₆), δ : 3.66 (m, 16 H, CH₂, thf); 2.24 and 2.13 (both br.s, 2 H each, CH_{carb}); 1.51 (m, 16 H, CH₂, thf); 1.30 and 1.29 (both s, 6 H each, SMe₂); −2.30 (br.s, 2 H, B—H—Na). ¹¹B NMR (C₆D₆), δ : −3.73 (d, 2 B, J = 143 Hz); −7.52 (s, 2 B); −10.87 (d, 2 B, J = 154 Hz); −15.88 (d, 2 B, J = 162 Hz); −17.85 (d, 2 B, J = 165 Hz); −23.03 (d, 2 B, J = 153 Hz); −25.51 (d, 2 B, J = 144 Hz); −29.27 (d, 2 B, J = 132 Hz); −35.65 (d, 2 B, J = 145 Hz).

Colorless crystals of compound **1** were grown by slow diffusion of light petroleum into a solution of compound **1** in THF in an NMR tube. At 110 K, crystals of **1** are monoclinic, space group $P2_1/n$, a = 13.678(2) Å, b = 9.637(1) Å, c = 15.356(2) Å, β = 96.023(6)°, V = 2013.0(5) Å³, Z = 4, d_{calc} = 1.190 g cm^{−3}, $\mu(\text{MoK}\alpha)$ = 1.85 cm^{−1}, $F(000)$ = 768. The intensities of 37155 reflections were measured at 110 K on a SMART 1000 CCD diffractometer ($\lambda(\text{MoK}\alpha)$ = 0.71072 Å, ω scanning mode, $2\theta < 100^\circ$), and 14353 independent reflections (R_{int} = 0.0296) were used in the refinement. The X-ray data were processed and merged using the SAINT Plus³⁰ and SADABS³¹ program packages.

The structure was solved by direct methods with the use of successive electron density maps. All hydrogen atoms were revealed from difference electron density maps. The structure was refined against F^2_{hkl} with anisotropic displacement parameters for all nonhydrogen atoms and isotropic displacement parameters for hydrogen atoms.

The final R factors for **1** were as follows: R_1 = 0.0409 (calculated based on F_{hkl} for 9230 reflections with $I > 2\sigma(I)$), wR_2 = 0.0925 (calculated based on F^2_{hkl} for all 14353 reflections), the number of parameters in the refinement was 354, GOF = 1.043. The calculations were carried out using the SHELXTL 5.10 program package.³²

The experimental electron density distribution function was determined in the analytical form by the multipole refinement of X-ray diffraction data in terms of the Hansen—Coppens model³³ using the XD program package.³⁴ In the multipole refinement, the coordinates, anisotropic displacement parameters, and the multipole parameters up to the octupole level ($l = 3$) were refined for all nonhydrogen atoms against F_{hkl} . The positions of the hydrogen atoms and their isotropic displacement parameters remained fixed. Before the refinement, all C—H distances were normalized to the ideal distance (1.08 Å). The B—H distances were calculated by the quantum-chemical method (PBE/TZ2p). In the multipole refinement, the H atoms were refined up to the dipole level ($l = 2$) taking into account the cylindrical symmetry. The correctness of the anisotropic atomic displacement parameters was estimated using the Hirshfeld test,³⁵ which was at most $10 \cdot 10^{-4}$ Å² for the bonds of the *nido*-carborane cage. The results of the multipole refinement are characterized by the following parameters: R = 0.0318, wR = 0.0306, GOF = 1.104 for 8548 reflections with $I > 3\sigma(I)$.

The potential energy density $v(\mathbf{r})$ was calculated from X-ray diffraction data using an approximation in terms of the Thomas—Fermi theory.³⁶ According to this approach, the kinetic energy density $g(\mathbf{r})$ can be calculated from the equation

$$g(\mathbf{r}) = 3/10(3\pi^2)^{2/3}[\rho(\mathbf{r})]^{5/3} + (1/72)|\nabla\rho(\mathbf{r})|^2/\rho(\mathbf{r}) + 1/6\nabla^2\rho(\mathbf{r})$$

combined with the local virial theorem⁵ ($2g(\mathbf{r}) + v(\mathbf{r}) = 1/4\nabla^2\rho(\mathbf{r})$), which allows calculations of both the potential energy density and the local energy density $h_{\text{e}}(\mathbf{r})$. The CPs (3,−1)

were found and the corresponding topological characteristics of $\rho(\mathbf{r})$, including $h_c(\mathbf{r})$, $g(\mathbf{r})$, and $v(\mathbf{r})$, were calculated using the WINXPRO 1.5.20 program.³⁷

Quantum-chemical calculations for anion **2** and dianion **3** were performed using the GAUSSIAN-98 program³⁸ with the B3LYP functional and the 6-31+G** basis set. The geometry optimization of Na...H—B-bonded dimer of **1** was carried out using the PRIRODA program³⁹ (PBE/TZ2P). The electron density function was determined from the results of B3LYP/6-311G** calculations of the energy using the geometry evaluated at the PBE/TZ2P level of theory. The topological analysis of the calculated function $\rho(\mathbf{r})$ was performed using the MORPHY 98 program.⁴⁰

This study was financially supported by the Russian Foundation for Basic Research (Project No. 03-03-32214) and the Foundation of the President of the Russian Federation (Federal Programs for the Support of Leading Scientific Schools, Grant NSh 1060.2003.03, and the Program for Support of Young Doctors, Grant MK-1209.2003.03).

References

1. K. A. Lyssenko, D. V. Lyubetskii, A. B. Sheremetev, and M. Yu. Antipin, *Izv. Akad. Nauk, Ser. Khim.*, 2005, 903 [*Russ. Chem. Bull., Int. Ed.*, 2005, **54**, 924].
2. M. F. Hawthorne, D. C. Young, T. D. Andrews, D. V. Howe, R. L. Pilling, A. D. Pitts, M. A. Reintjes, L. F. Warren, and P. A. Wegner, *J. Am. Chem. Soc.*, 1968, **90**, 879.
3. A. K. Saxena and N. S. Hosmane, *Chem. Rev.*, 1993, **93**, 1081.
4. A. K. Saxena, J. A. Maguire, and N. S. Hosmane, *Chem. Rev.*, 1993, **93**, 1081.
5. R. N. Grimes, in *Comprehensive Organometallic Chemistry II*, Eds E. W. Abel, F. A. G. Stone, and G. Wilkinson, Pergamon, Oxford, 1995, **1**, 373.
6. V. I. Mesheryakov, K. A. Lyssenko, G. V. Grintselev-Knyazev, P. V. Petrovskii, and A. R. Kudinov, in *Boron Chemistry at the Beginning of the 21st Century*, Ed. Yu. N. Bubnov, Moscow, 2003, 255.
7. G. Zi, H.-W. Li, and Z. Xie, *Organometallics*, 2001, **20**, 3836.
8. M. A. Fox, A. K. Hughes, A. L. Johnson, and M. A. J. Paterson, *J. Chem. Soc., Dalton Trans.*, 2002, 2009.
9. G. D. Kolomnikova, P. V. Petrovskii, P. V. Sorokin, F. M. Dolgushin, A. I. Yanovsky, and I. T. Chizhevsky, *Izv. Akad. Nauk, Ser. Khim.*, 2001, 677 [*Russ. Chem. Bull., Int. Ed.*, 2001, **50**, 706].
10. I. T. Chizhevsky, A. I. Yanovsky, and Yu. T. Struchkov, *J. Organomet. Chem.*, 1997, **536**, 51.
11. (a) J. A. Long, T. B. Marder, P. E. Behnken, and M. F. Hawthorne, *J. Am. Chem. Soc.*, 1984, **106**, 2979; (b) C. B. Knobler, T. B. Marder, E. A. Mizusawa, R. G. Teller, J. A. Long, P. E. Behnken, and M. F. Hawthorne, *J. Am. Chem. Soc.*, 1984, **106**, 2990.
12. L. A. Leites, *Chem. Rev.*, 1992, **92**, 279.
13. R. F. W. Bader and D. A. Legarre, *Can. J. Chem.*, 1992, **70**, 657.
14. K. A. Lyssenko, M. Yu. Antipin, and V. N. Lebedev, *Inorg. Chem.*, 1998, **37**, 5834.
15. I. V. Glukhov, K. A. Lyssenko, A. A. Korlyukov, and M. Yu. Antipin, *Izv. Akad. Nauk, Ser. Khim.*, 2005, 541 [*Russ. Chem. Bull., Int. Ed.*, 2005, **54**, 547].
16. N. S. Hosmane, A. K. Saxena, R. D. Baretto, H. Zhang, J. A. Maguire, L. Jia, Y. Wang, A. R. Oki, K. V. Grover, S. J. Witten, K. Dawson, M. A. Tolle, U. Siriwardane, T. Demissie, and J. S. Fagner, *Organometallics*, 1993, **12**, 3001.
17. N. S. Hosmane, J. Yang, H. Zhang, and J. A. Maguire, *J. Am. Chem. Soc.*, 1996, **118**, 5150.
18. R. F. W. Bader, *Atoms in Molecules. A Quantum Theory*, Clarendon Press, Oxford, 1990.
19. J. Cowie, E. J. M. Hamilton, J. C. V. Laurie, and A. J. Welch, *J. Organomet. Chem.*, 1990, **394**, 1.
20. A. A. Korlyukov, K. A. Lyssenko, and M. Yu. Antipin, *Izv. Akad. Nauk, Ser. Khim.*, 2002, 1314 [*Russ. Chem. Bull., Int. Ed.*, 2002, **51**, 1423].
21. A. A. Korlyukov, K. A. Lyssenko, M. Yu. Antipin, V. N. Kirin, E. A. Chernyshev, and S. P. Knyazev, *Inorg. Chem.*, 2002, **41**, 5043.
22. V. Jonas, G. Frenking, and M. T. Reed, *J. Am. Chem. Soc.*, 1994, **116**, 8741.
23. J. Cowie, E. J. M. Hamilton, J. C. V. Laurie, and A. J. Welch, *Acta Crystallogr.*, 1988, **C48**, 1648.
24. A. R. Kudinov, D. S. Perekalin, P. V. Petrovskii, K. A. Lyssenko, G. V. Grintselev-Knyazev, and Z. A. Starikova, *J. Organomet. Chem.*, 2002, **657**, 115.
25. A. S. F. Boyd, G. M. Rosair, F. B. H. Tiarks, A. S. Weller, S. K. Zahn, and A. J. Welch, *Polyhedron*, 1998, **17**, 2627.
26. (a) M. Yu. Antipin, K. A. Lyssenko, and R. Boese, *J. Organomet. Chem.*, 1996, **508**, 259; (b) K. A. Lyssenko, M. Yu. Antipin, and C. Yu. Ketkov, *Izv. Akad. Nauk, Ser. Khim.*, 2001, 125 [*Russ. Chem. Bull., Int. Ed.*, 2001, **50**, 130].
27. K. A. Lyssenko, D. G. Golovanov, and M. Yu. Antipin, *Mendeleev Commun.*, 2003, 209.
28. E. Espinosa, E. Mollins, and C. Lecomte, *Chem. Phys. Lett.*, 1998, **285**, 170.
29. K. A. Lyssenko and M. Yu. Antipin, *Izv. Akad. Nauk, Ser. Khim.*, 2004, 11 [*Russ. Chem. Bull., Int. Ed.*, 2004, **53**, 10].
30. SMART. Bruker Molecular Analysis Research Tool, v. 5.059, Bruker AXS, Madison, Wisconsin, USA, 1998.
31. G. M. Sheldrick, *SADABS*, Bruker AXS Inc., Madison, WI-53719, USA, 1997.
32. G. M. Sheldrick, *SHELXTL-97, Version 5.10*, Bruker AXS Inc., Madison, WI-53719, USA, 1998.
33. N. K. Hansen and P. Coppens, *Acta Crystallogr.*, 1978, **34A**, 909.
34. T. Koritsanszky, S. T. Howard, T. Richter, P. Macchi, A. Volkov, C. Gatti, P. R. Mallinson, L. J. Farrugia, Z. Su, and N. K. Hansen, *XD — A Computer Program Package for Multipole Refinement and Topological Analysis of Charge Densities from Diffraction Data*, 2003.
35. F. L. Hirshfeld, *Acta Crystallogr.*, 1976, **32A**, 239.
36. D. A. Kirzhnits, *Zh. Eksp. Teor. Fiz.*, 1957, **5**, 64 [*J. Exp. Theor. Phys. USSR*, 1957, **5**, 64 (Engl. Transl.)].
37. A. Stash and V. Tsirelson, *WinXPRO — a Program for Calculation of the Crystal and Molecular Properties Using The*

- Model Electron Density*, Moscow (Russia), 2001; <http://xray.nifhi.ru/wxp/>
38. M. J. Frisch, G. W. Trucks, H. B. Schlegel, G. E. Scuseria, M. A. Robb, J. R. Cheeseman, V. G. Zakrzewski, J. A. Montgomery, Jr., R. E. Stratmann, J. C. Burant, S. Dapprich, J. M. Millam, A. D. Daniels, K. N. Kudin, M. C. Strain, O. Farkas, J. Tomasi, V. Barone, M. Cossi, R. Cammi, B. Mennucci, C. Pomelli, C. Adamo, S. Clifford, J. Ochterski, G. A. Petersson, P. Y. Ayala, Q. Cui, K. Morokuma, D. K. Malick, A. D. Rabuck, K. Raghavachari, J. B. Foresman, J. Cioslowski, J. V. Ortiz, A. G. Baboul, B. B. Stefanov, G. Liu, A. Liashenko, P. Piskorz, I. Komaromi, R. Gomperts, R. L. Martin, D. J. Fox, T. Keith, M. A. Al-Laham, C. Y. Peng, A. Nanayakkara, M. Challacombe, P. M. W. Gill, B. Johnson, W. Chen, M. W. Wong, J. L. Andres, C. Gonzalez, M. Head-Gordon, E. S. Replogle, and J. A. Pople, *GAUSSIAN-98, Revision A.9*, Gaussian, Inc., Pittsburgh (PA), 1998.
39. D. N. Laikov, *Chem. Phys. Lett.*, 1997, **281**, 151.
40. (a) P. L. A. Popelier, *MORPHY98, Comp. Phys. Commun.*, 1996, **93**, 212; (b) P. Popelier, *Chem. Phys. Lett.*, 1994, **228**, 160.

Received December 1, 2004;
in revised form March 29, 2005